

# Supplementary Information; Liquid-liquid equilibrium in polymer- fullerene mixtures; an *in-situ* neutron reflectivity study

E. L. Hynes<sup>1</sup>, P. Gutfreund<sup>2</sup>, A. J. Parnell<sup>3</sup>, A. M. Higgins<sup>1\*</sup>

<sup>1</sup> College of Engineering, Swansea University, Bay Campus, Fabian Way, Swansea SA1 8EN, Wales, United Kingdom

<sup>2</sup> Institut Laue-Langevin, 71 avenue des Martyrs, 38000 Grenoble, France

<sup>3</sup> Department of Physics and Astronomy, The University of Sheffield, Sheffield S3 7RH, United Kingdom

\* Corresponding author - [a.m.higgins@swansea.ac.uk](mailto:a.m.higgins@swansea.ac.uk)

## Sample fabrication

Table S1 shows the solution concentrations and spin-coating speeds used for the PS and fullerene layers in this study.

Layer	Thickness (from NR fits to bilayers before annealing) (Å)	Concentration (weight%)	Spin speed (RPM)
PCBM	218	1.5	3000
Bis-PCBM	222	1.5	3000
2k-PS	622	2.5	3000
3k-PS	621	2.5	3000
5k-PS	510	2	2000
20k-PS	402	1.5	2000
100k-PS	520	1.5	1500

**Table S1: Solution concentrations and spin-coating speeds used to fabricate the individual layers within the bilayer samples.** The PCBM and bis-PCBM were dissolved in chlorobenzene and the PS was dissolved in toluene.

## NR on single layer samples

Figures S1 and S2 show NR measurements on PS and PCBM single layers during heating and cooling. The PS film shows behaviour that corresponds to the known thermal expansion/contraction on heating/cooling. This can be seen in fig. S3a, in which the thickness versus time data from fig. S2a is converted into thickness versus sample (surface) temperature (using the measured cooling rates in fig. S6 at a set-point of 30°C; i.e. as the sample gradually cools), and shows reasonable agreement with the reported thermal expansivity of PS thin films<sup>1</sup>. The PCBM film shows very little change in thickness over the temperature range investigated in our study; changes in thickness up to a set-point of 160 °C are less than 1% (the changes in the PCBM film at a set-point of 180 °C are due to significant roughening of the film surface, probably associated with crystallisation of this particular sample).

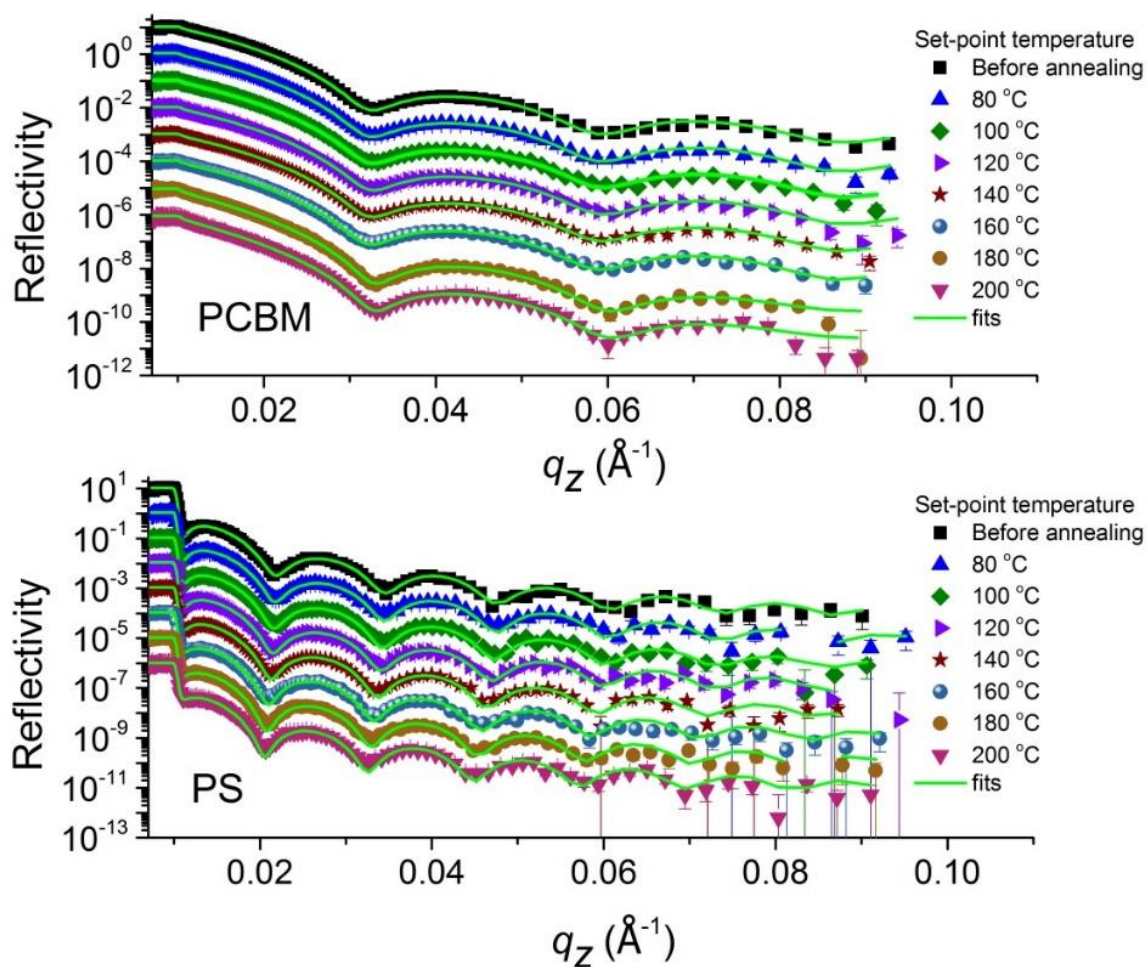


**Fig S1; Kinetic measurements of the reflectivity curve for a PCBM single layer, and a 20k-PS single layer.** Each curve corresponds to a time slice of 2.5 min that begins 2.5 min after the temperature was changed to the set-point shown in the legend.

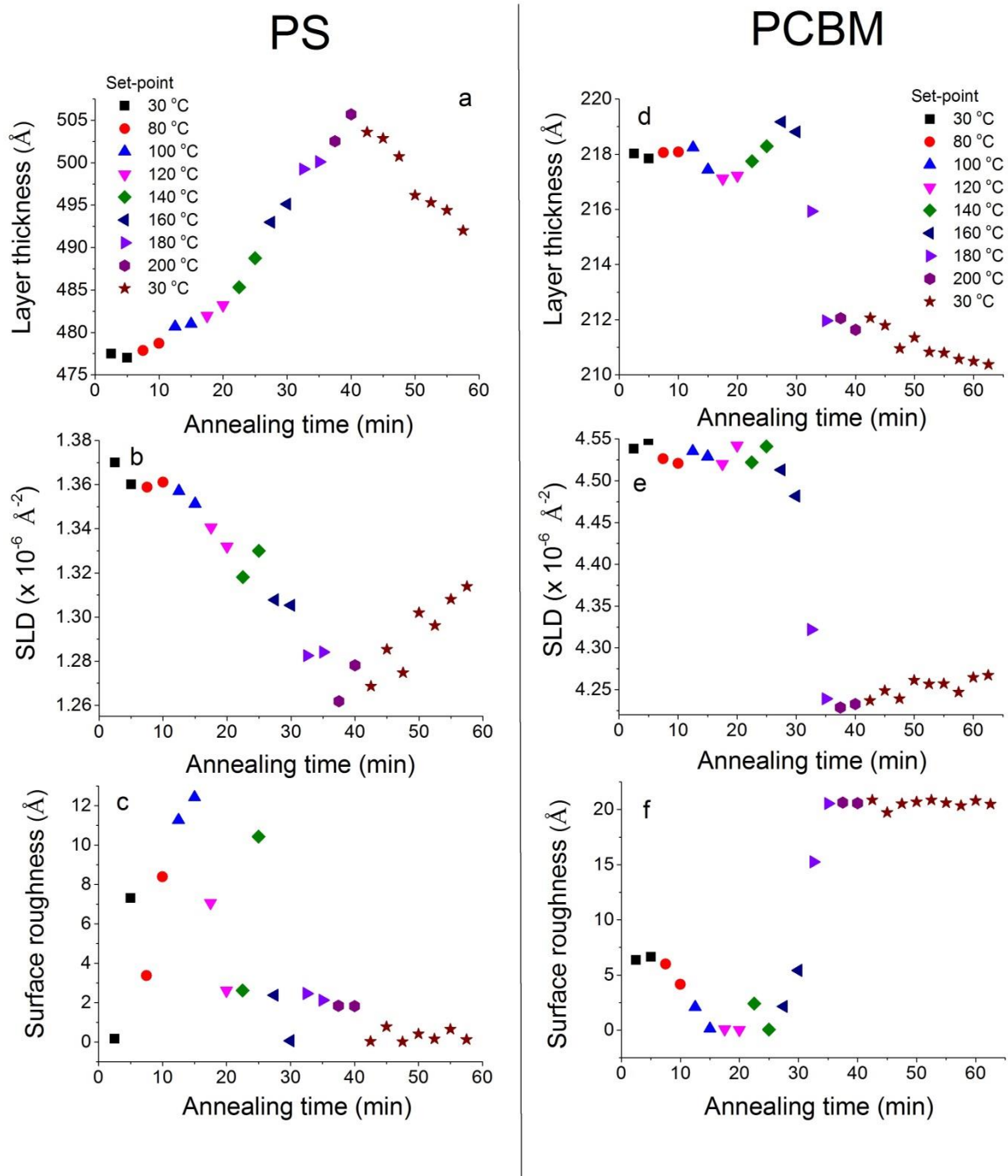


**Fig S2: Single layer fit parameters versus time during heating and cooling;** a), b), c) Layer thickness, SLD and surface roughness respectively for a 20k-PS single layer. d), e), f) Layer thickness, SLD and surface roughness respectively for a PCBM single layer. Each data point represents the fit to the reflectivity summed over five (consecutive) 30s measurements. The filled star symbols labelled 30 °C, represent measurements performed during gradual cooling of the samples at the end of annealing.

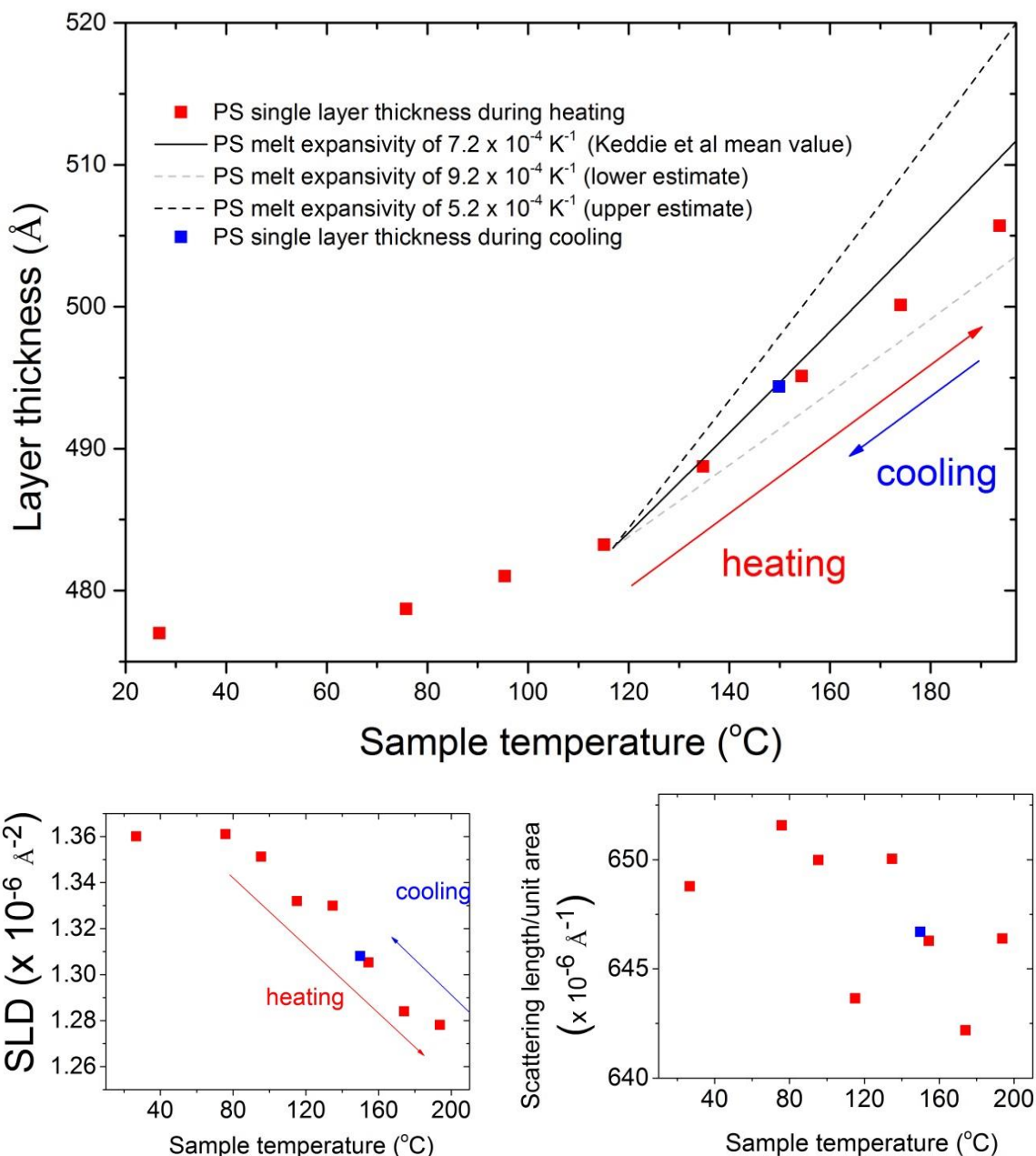


**Fig S3; 20k-PS single layer changes as a function of sample temperature during heating and cooling;** a) Thickness changes in comparison to the thermal expansivity from literature<sup>1</sup>, b) SLD, c) Scattering length per unit area (the product of the data in a and b). The data points shown correspond to neutrons collected between 2.5 and 5 min at the specified temperature (i.e. for each set-point temperature in fig. S2, this is the data point at the longer annealing time). NB; The equilibrated melt expansivity lines in a) are plotted from 390K (117 °C) onwards, as this is the temperature which PS thin-films need to reach on first heating before they reversibly follow the equilibrated melt expansivity<sup>1</sup>.

## Sensitivity to roughness parameters

Figure S4 shows a contour plot for the goodness of fit,  $\chi^2$ , parameter versus the sample surface roughness and the interfacial roughness. The contour plot shows a single well-defined approximately elliptically-shaped minimum. The long axis of the ellipse is approximately 2.5 times longer than the short axis, indicating the greater sensitivity of the model to the interfacial roughness in comparison to the sample surface roughness.

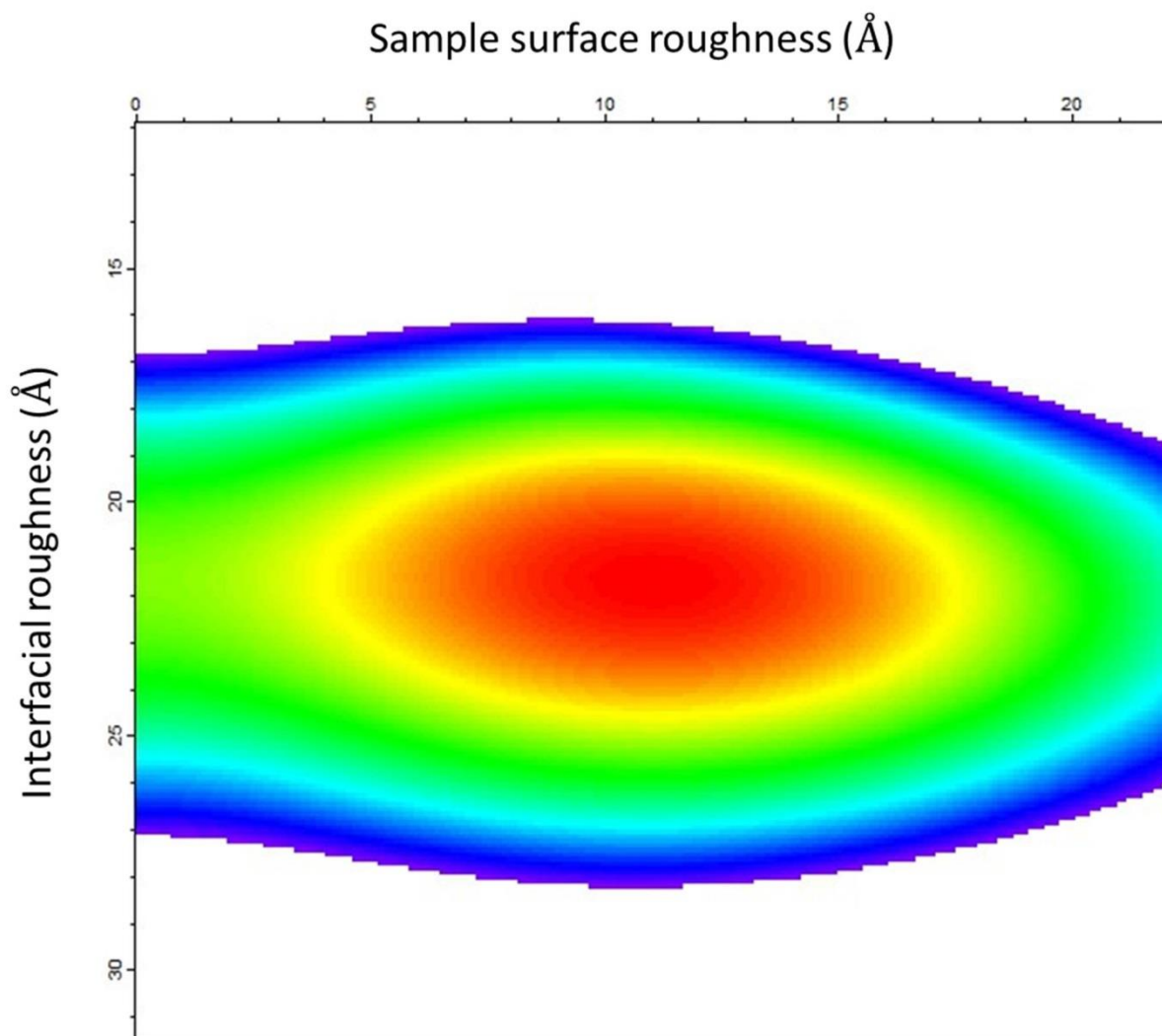


**Figure S4; Goodness of fit parameter,  $\chi^2$ , contour map as function of the surface and interfacial roughness fit parameters.** The map corresponds to a bilayer model of the full reflectivity curve (out to  $q_z=0.2 \text{ \AA}^{-1}$ ) after annealing, for the PCBM/5k-PS bilayer shown in fig. 1d. The minimum in  $\chi^2$  (fitted by letting all six adjustable parameters in the bilayer model vary) is located at surface and interfaces roughnesses of 11 Å and 22 Å respectively. The full range of contours shown represents a doubling of the  $\chi^2$  values from the minimum value (of 9.2).

## Temperature control

*In-situ* annealing was carried out by bolting the silicon wafers to the surface of a heater (see fig. S7a) inside a vacuum chamber with quartz windows, that was placed in the neutron beam. Temperature calibration (see figs S5 and S6) at the sample surface was performed before the

NR measurements were taken, using a k-type thermocouple attached to the surface of a duplicate silicon wafer. For the calibration, the samples were bolted to the heater tightly. When we came to perform the NR experiment, we found that such tight attachment had the effect of causing some wafers to bend very slightly (detected as a broadening of the reflected beam on the detector), and therefore the NR experiments were performed with less tight bolting. After the experiment, the calibration was therefore repeated using different tightness levels of the bolting, corresponding to the values used in the NR measurements (low-medium bolting tightness). The results of this calibration (see fig. S7b) show that the samples had a slightly lower temperature than when tightly bolted (between around 1 and 4 °C), giving an uncertainty in the sample (surface) temperatures due to the tightness of the bolting of  $\pm 1.5$  °C. This is within the accuracy of the thermocouple (which is  $\pm 2.2$  degrees). The mean stabilised sample temperatures for each set-point are given in table S2.

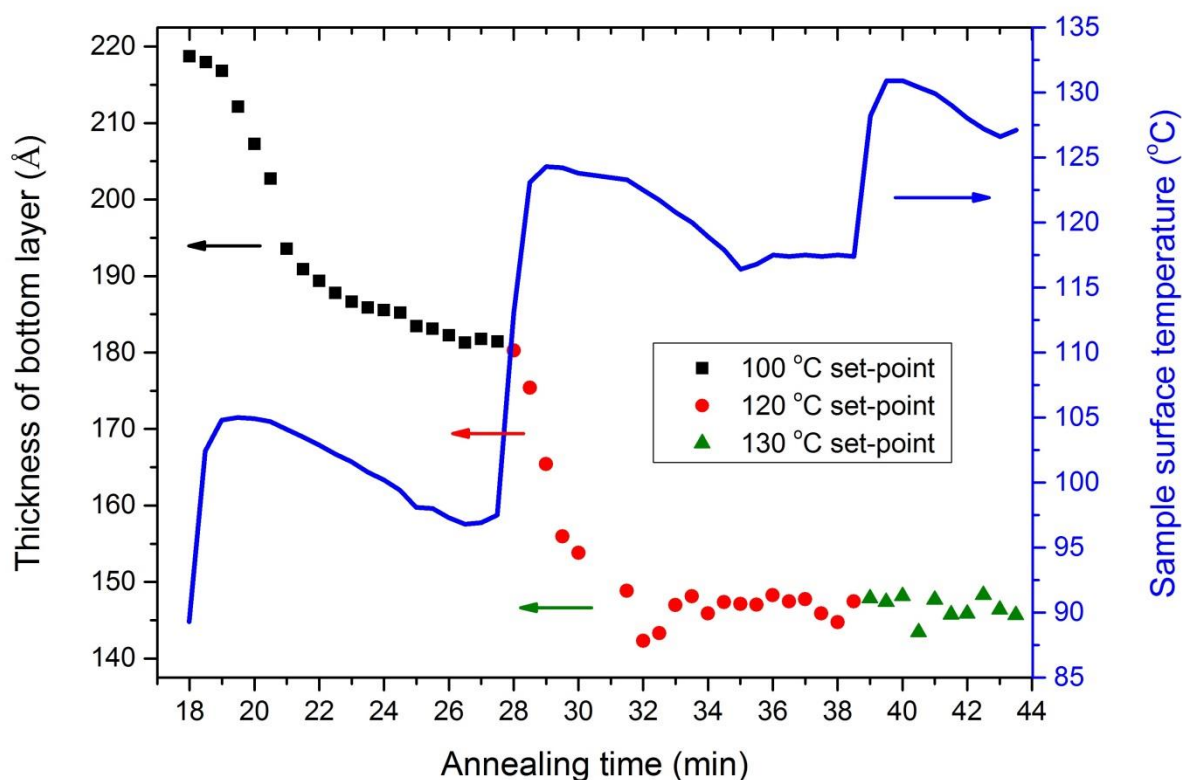


**Fig S5; The temperature of the sample surface and the thickness of the bottom (PCBM) layer versus annealing time, for the PCBM/3k-PS bilayer.** The thickness parameters (shown as discrete points) are from fits to 30 s slices. The sample (surface) temperature is shown as a continuous blue curve.

Set-point (°C)	80	100	120	130	140	150	160	180
Sample (surface) temperature (°C)	76	95	115	125	135	145	154	174

**Table S2: Set-point and (stabilised) mean sample temperature for *in-situ* annealed samples.** The mean sample temperature is taken as the mid-point between that of a sample that is attached to the heater with low tightness and medium tightness.

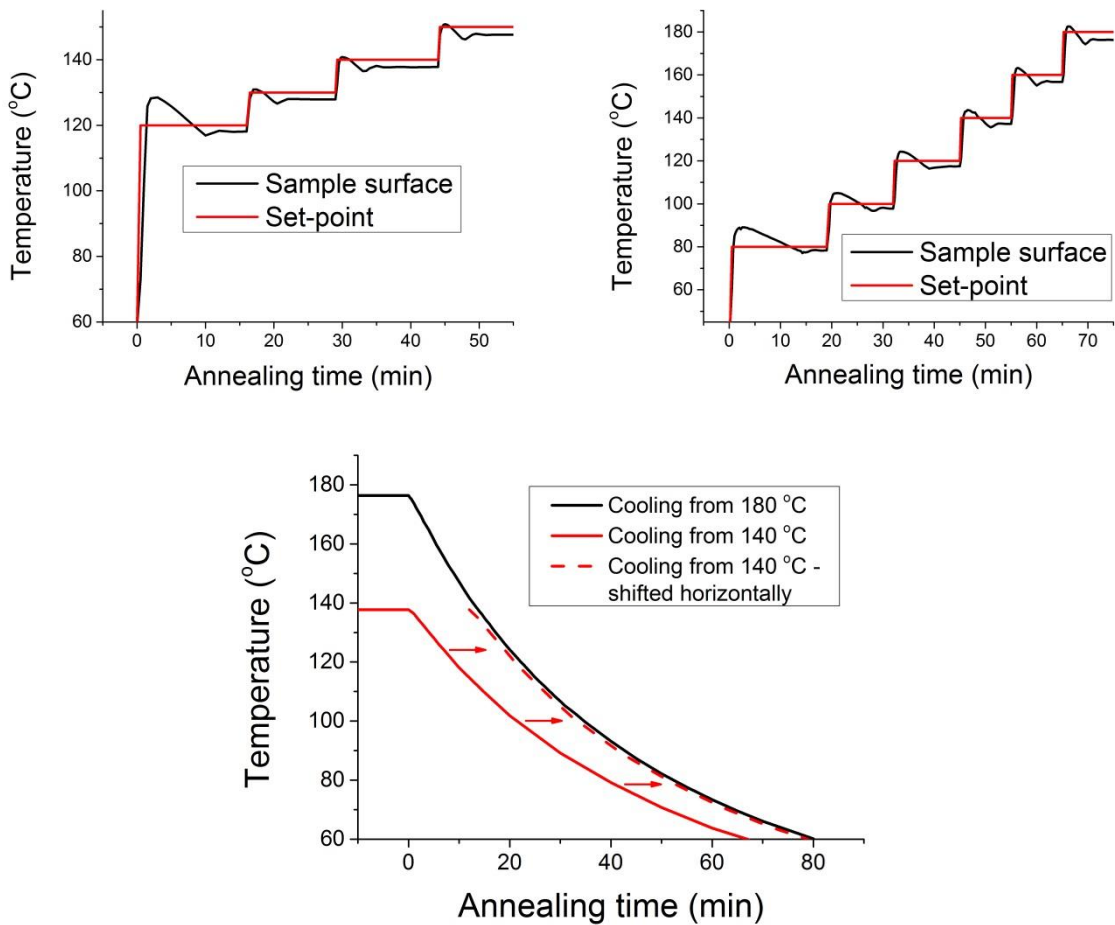


**Fig S6; Sample temperatures and set-point temperatures versus time for the calibration sample.** a) For a 60 °C step followed by 10 °C steps; b) For a 35 °C step followed by 20 °C steps. c) Sample temperatures on cooling from set-points of 180 °C and 140 °C. The sample was tightly bolted (referred to as ‘high tightness’ in fig. 7b) to the heater for these measurements.

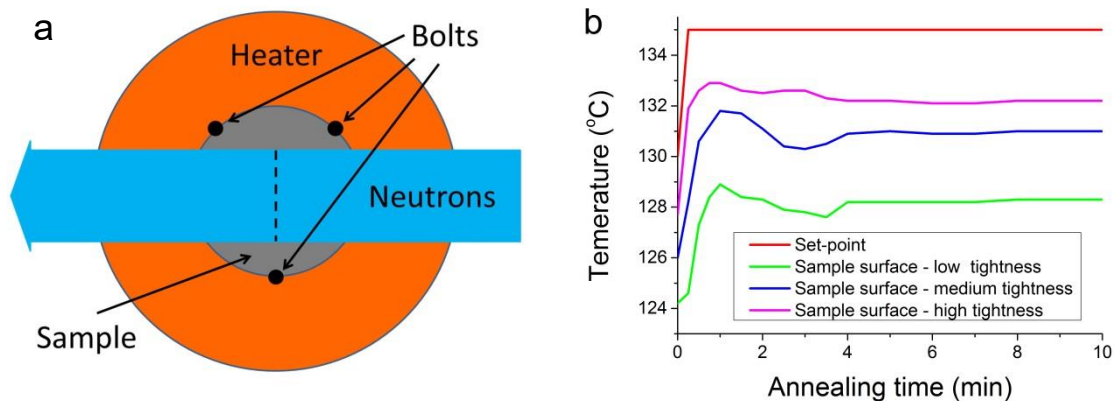


**Fig S7; a) Schematic diagram (plan view) showing how the samples were attached to the heating stage during the *in-situ* measurements; b) Sample temperature versus time as a function of how tightly the sample was bolted onto the heating stage. During neutron scattering measurements the sample were attached in the range between low and medium tightness.**

## Robustness of NR fit parameters

Figures S8a-e show the six adjustable fit parameters for kinetic measurements of the 2k-PS/PCBM sample in 30s time slices. Comparison of these plots with figs 3a-c and S8f-g, which show fit parameters for 2 min time slices for the same sample, show good agreement.

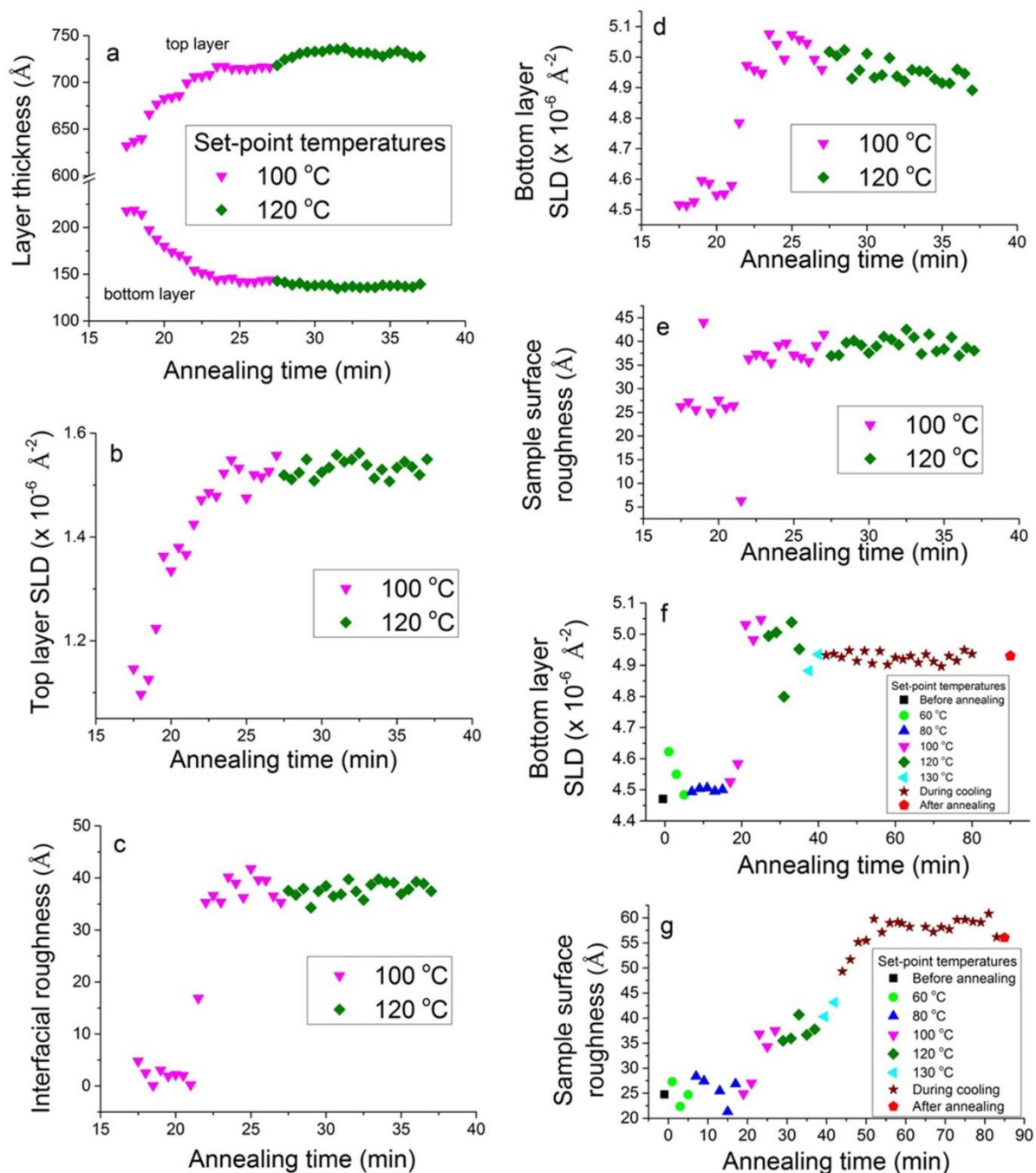


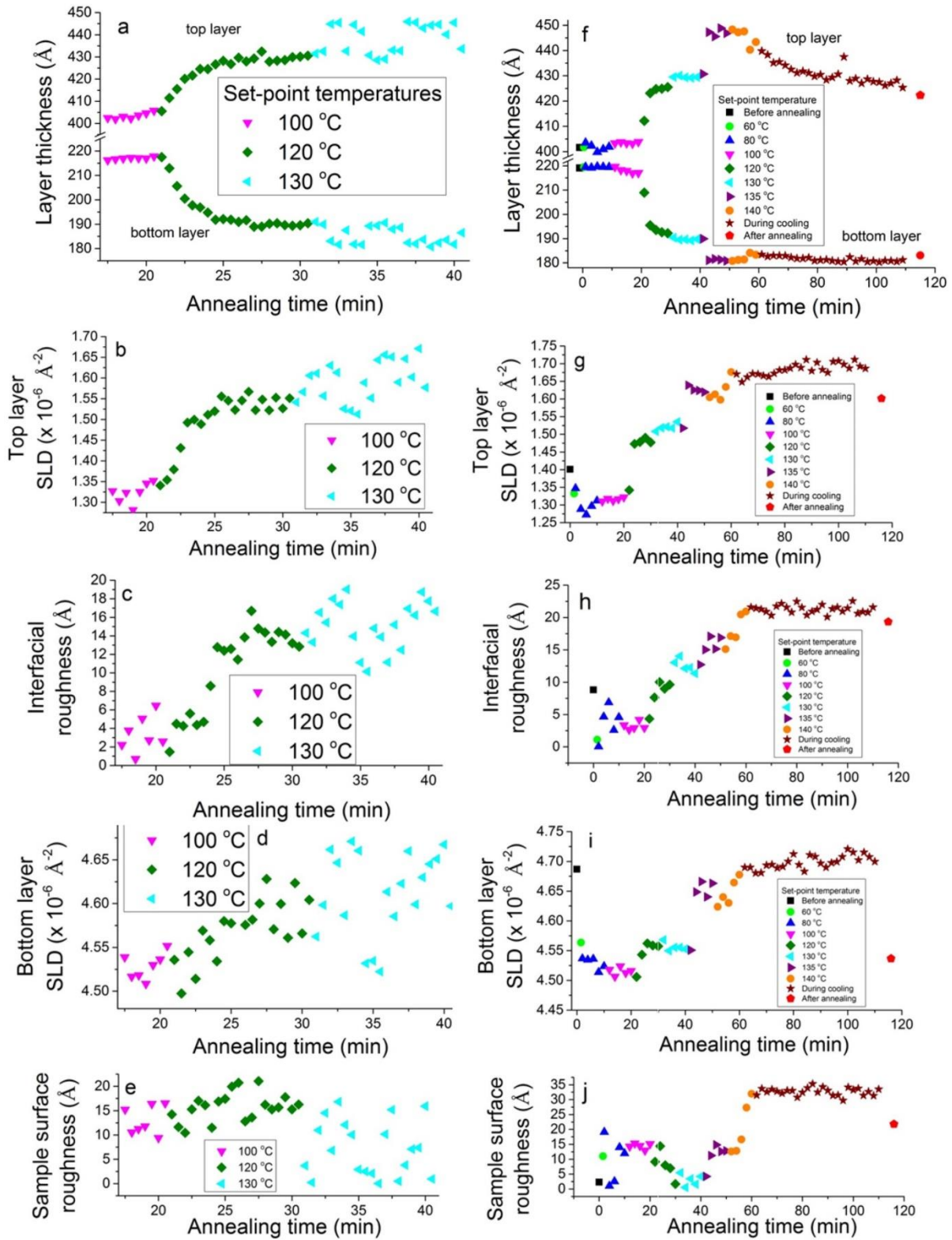
**Fig S8; PCBM/2k-PS fit parameters versus time (6 adjustable parameters in all fits);** a) Top and bottom layer thickness; b) Top layer SLD; c) Interfacial roughness; d) Bottom layer SLD; e) Sample surface roughness; f) Bottom layer SLD; g) Sample surface roughness. The parameters in f) and g) accompany the other 4 fit parameters that are shown in figs 3a-3c in the main paper. The kinetic fit parameters in a)-e) correspond to 30s time slices and in f)-g) correspond to 2 min time slices.

Figures S9a-e show the fit parameters for kinetic measurements of the 20k-PS/PCBM sample in 30s time slices, in which all six parameters are adjustable. These plots and figs S9f-j, which

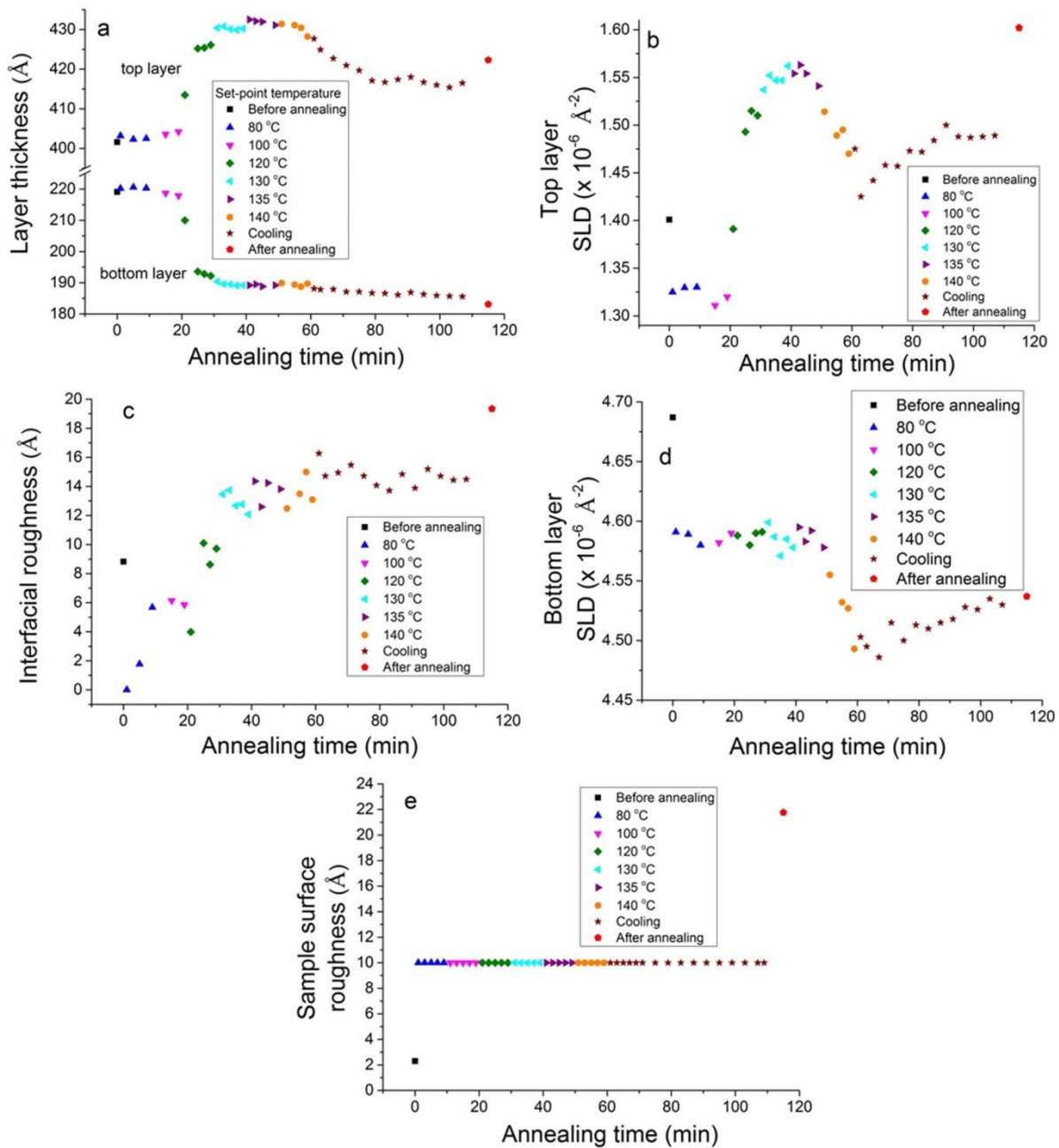
show fit parameters for 2 min time slices for the same sample, show behaviour that indicates that six adjustable parameters is too many for this particular sample to converge on a unique solution. This is most clearly demonstrated in fig. S9a, in which it is clear that on changing the set-point to 130 °C, the layer thickness parameters jump between two discrete sets of values; when the top layer is thinner, the bottom layer is thicker and vice versa. This behaviour is not apparent at 130 °C in the 2 min time slice data (fig S9f), but sudden jumps in the layer thickness that are later reversed are still seen here; most notably shortly after the set-point is changed to 135 °C and near the end of the 140 °C set-point period.

Several different fitting approaches, in which the number of adjustable parameters for the 20k-PS/PCBM sample is restricted, are shown in figs S10, S11 and S12. In fig. S10 the sample surface roughness is fixed at 10 Å for the kinetic fits (a value intermediate between the value obtained from the full reflectivity curve measurements before and after annealing). In fig. S11 the sample surface roughness is fixed at 10 Å and the bottom layer SLD is fixed at  $4.65 \times 10^{-6} \text{Å}^{-2}$  (the mean value obtained for *ex-situ* annealed samples<sup>2,3</sup>, which is intermediate between the values obtained from the full reflectivity curve measurements before and after annealing on this sample). In fig. S12 just the bottom layer SLD is fixed (at  $4.65 \times 10^{-6} \text{Å}^{-2}$ ); the bottom layer SLD and the sample surface roughness are shown here, with the four key fit parameters for this sample shown in figs 3j-l. Examination of figs S10-S12 and fig. 3 show that there are some quantitative differences (most notably in terms of the values of the top layer thickness in fig. S10a at set-points of 130-140 °C, which are about 10 Å lower than in the other figs), but that the overall behaviour is robust with-respect-to the different fitting methodologies (in particular in terms of the onset temperatures for fullerene diffusion and the behaviour on cooling).

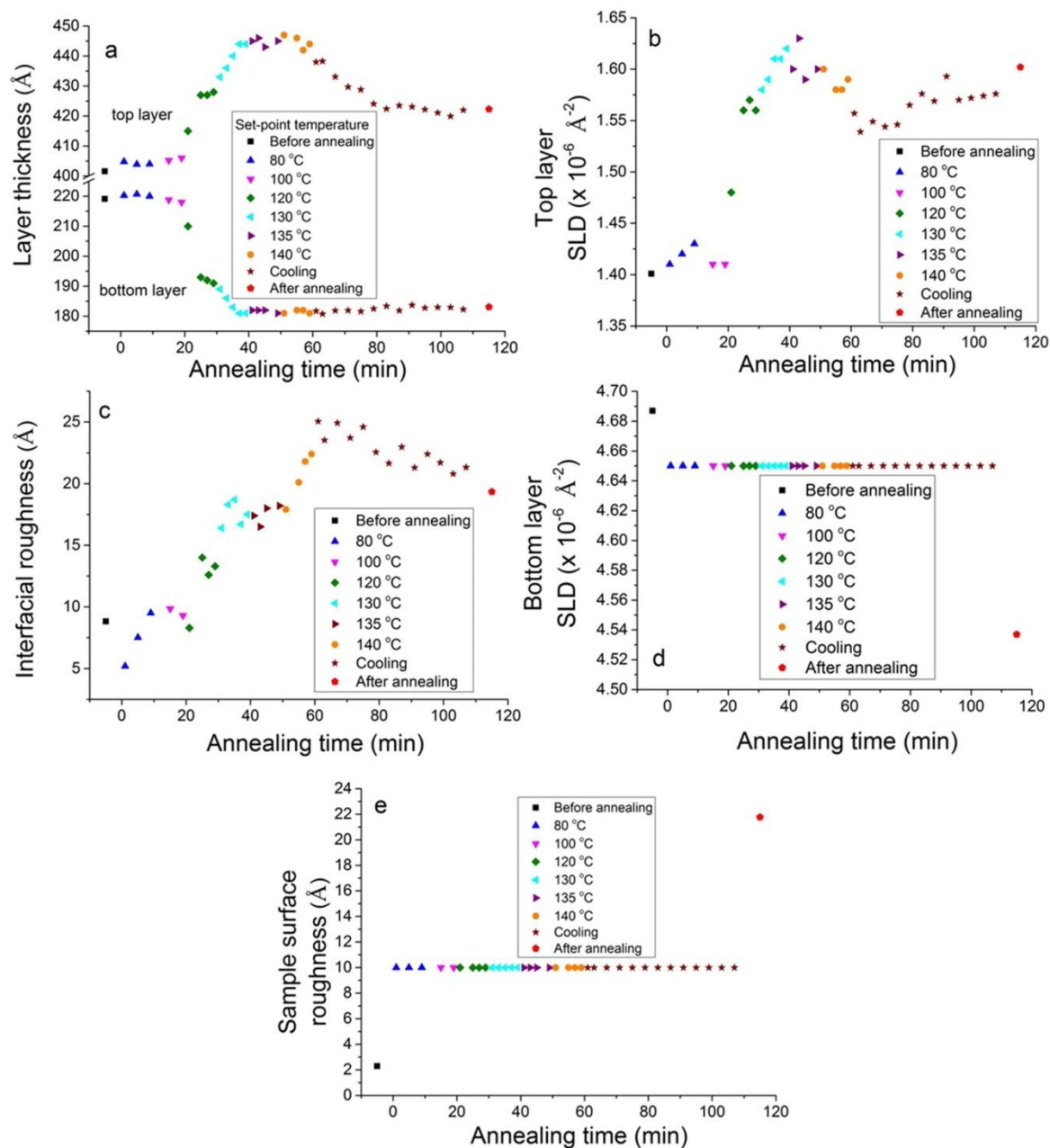
For completeness, figs S13 and S14 show the bottom layer SLD and the sample surface roughness for the 100k-PS/bis-PCBM and 5k-PS/PCBM samples respectively. These parameters accompany the key fit parameters shown in fig. 5 and figs 3g-i. Figure S14b shows that the sample surface roughness parameter for the kinetic fits appears to reduce to around zero when the set-point is raised to 120 °C. This behaviour is not reflected in the full reflectivity curves measured before and after annealing (in which the surface roughness remains at around 10 Å), and is potentially an artefact of the relative insensitivity of the fits to the sample surface roughness. In fig. S15 we examine this in further detail by comparing the kinetic fits for this sample in four different scenarios; i) in which we have six adjustable parameters, and ii)-iv) in which the sample surface roughness is fixed at 20, 0 and 10 Å (representing the approximate surface roughness parameters returned from the fits with six adjustable parameters, at set-points of below 120 °C, at set-points of 120 °C and above, and the mid-point of these two, respectively). It is clear from fig. S15 that the behaviour of the other five fit parameters is robust with-respect-to these values of the sample surface roughness, confirming (in conjunction with fig. S4) the relative insensitivity of the model to this parameter. A brief comment is required regarding the values obtained for the bottom layer SLD from the kinetic fits shown in fig S15d (and also elsewhere). These show a rapid increase in SLD after around 30 minutes that is not physically reasonable, as evidenced by the lack of any temperature dependence of the PCBM single layer data in figs S1 and S2, and the fact that any mixing with PS, were it to occur, would only *lower* the SLD. The behaviour in fig S15d is therefore clearly an artefact of the fitting, in which the bottom layer SLD if allowed to vary can show behaviour with time/temperature that correlates with the time/temperature-dependent behaviour of the other adjustable parameters. However, the actual SLD values in fig S15d are within the same range as that of the bottom layer (pure PCBM) SLDs found before and after annealing (full reflectivity curve fits) in the present study and also in our previous work<sup>3</sup>.



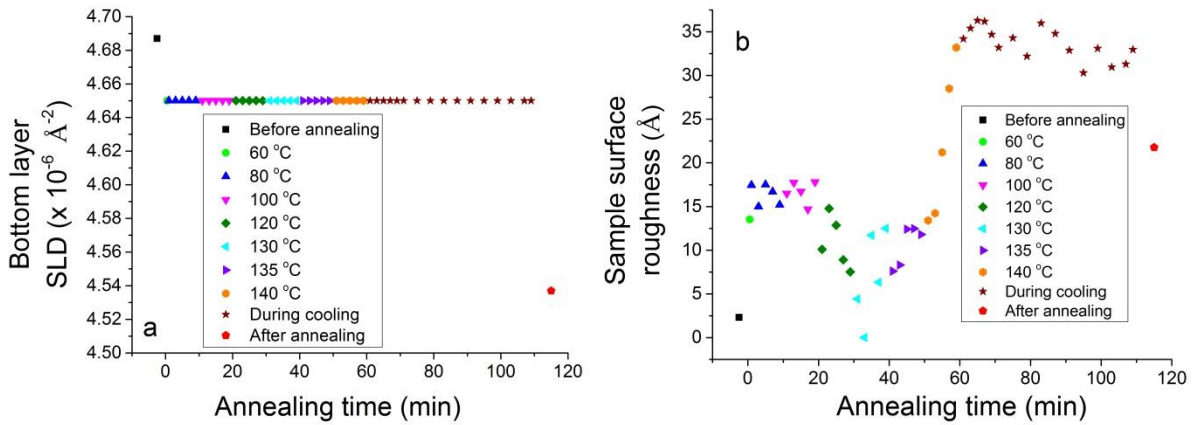
**Fig S9; PCBM/20k-PS fit parameters versus time (6 adjustable parameters in all fits);** a) Top and bottom layer thickness ; b) Top layer SLD; c) Interfacial roughness; d) Bottom layer SLD; e) Sample surface roughness; f) Top and bottom layer thickness; g) Top layer SLD; h) Interfacial roughness; i) Bottom layer SLD; j) Sample surface roughness. The kinetic fit parameters in a)-e) correspond to 30s time slices and in f)-j) correspond to 2 min time slices. The legend for S9j is the same as for S9f-i.



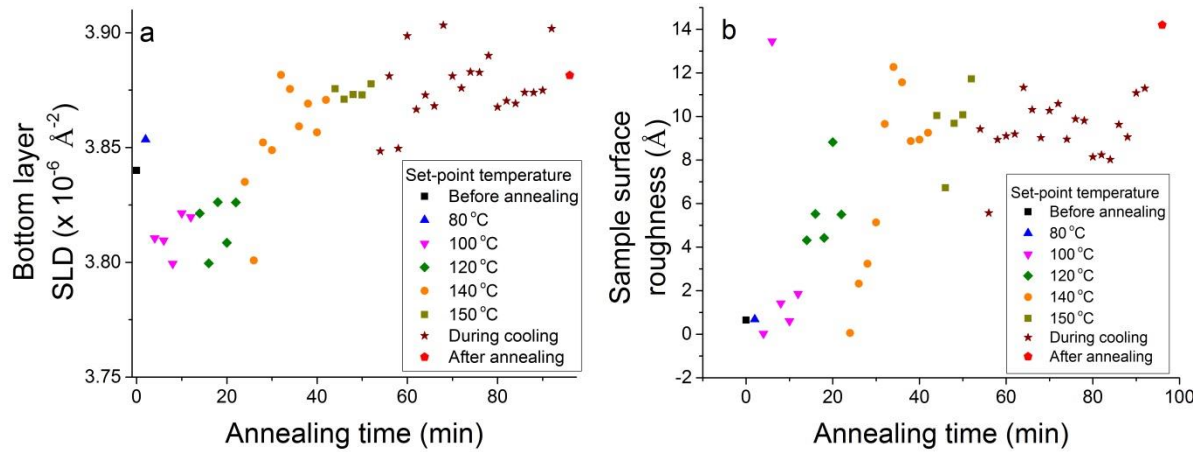
**Fig S10; PCBM/20k-PS fit parameters versus time (6 adjustable parameters in fits before and after annealing; sample surface roughness fixed at 10 Å during kinetic fits); a) Top and bottom layer thickness; b) Top layer SLD; c) Interfacial roughness; d) Bottom layer SLD; e) Sample surface roughness. The kinetic fit parameters all correspond to 2 min time slices.**



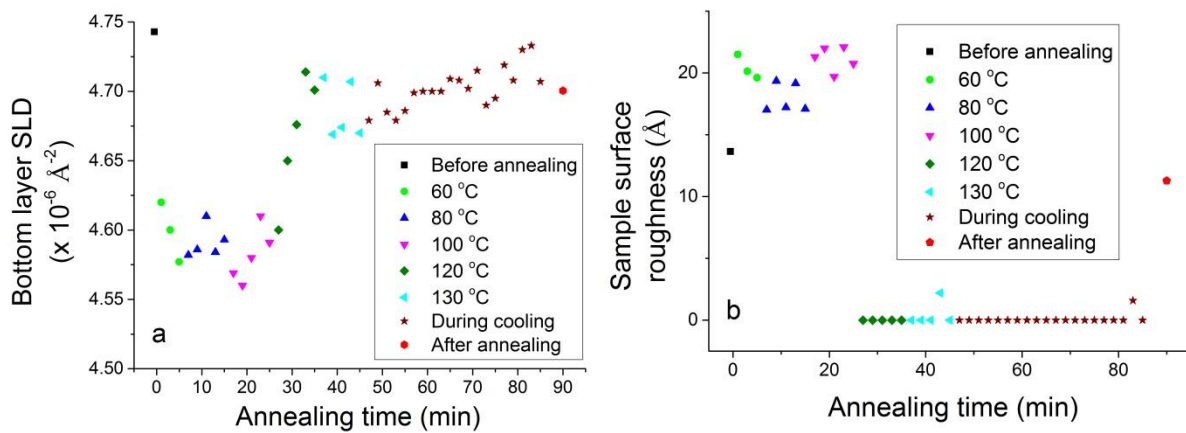
**Fig S11; PCBM/20k-PS fit parameters versus time (6 adjustable parameters in fits before and after annealing; sample surface roughness fixed at  $10 \text{ \AA}$  and bottom layer SLD fixed at  $4.65 \times 10^{-6} \text{ \AA}^{-2}$  during kinetic fits); a) Top and bottom layer thickness; b) Top layer SLD; c) Interfacial roughness; d) Bottom layer SLD; e) Sample surface roughness. The kinetic fit parameters all correspond to 2 min time slices.**



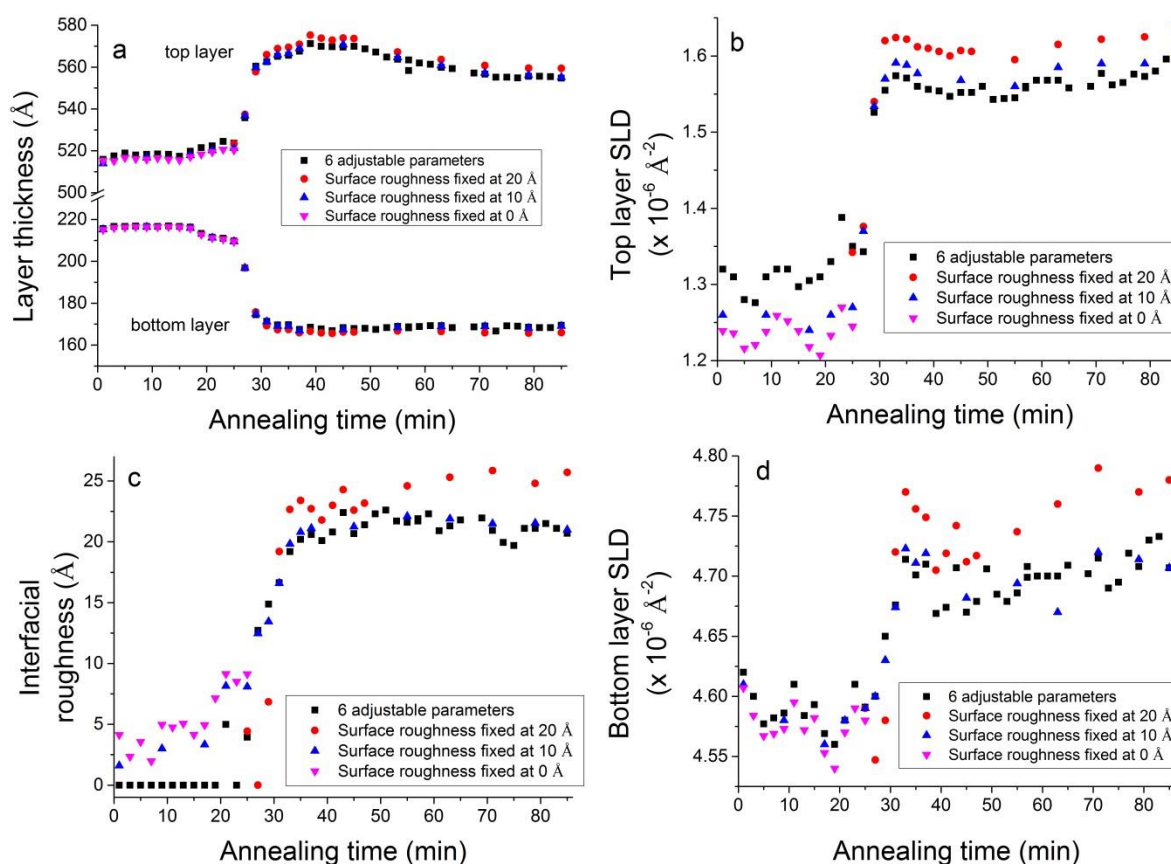
**Fig S12; PCBM/20k-PS fit parameters versus time (6 adjustable parameters in fits before and after annealing; bottom layer SLD fixed at  $4.65 \times 10^{-6} \text{ \AA}^{-2}$  during kinetic fits);** a) Bottom layer SLD; b) Sample surface roughness. The kinetic fit parameters all correspond to 2 min time slices. These parameters accompany the other four fit parameters that are shown in figs 3j-3l in the main paper.



**Fig S13; Bis-PCBM/100k-PS fit parameters versus time (6 adjustable parameters in all fits);** a) Bottom layer SLD; b) Sample surface roughness. The kinetic fit parameters all correspond to 2 min time slices. These parameters accompany the other four fit parameters that are shown in fig 5 in the main paper.



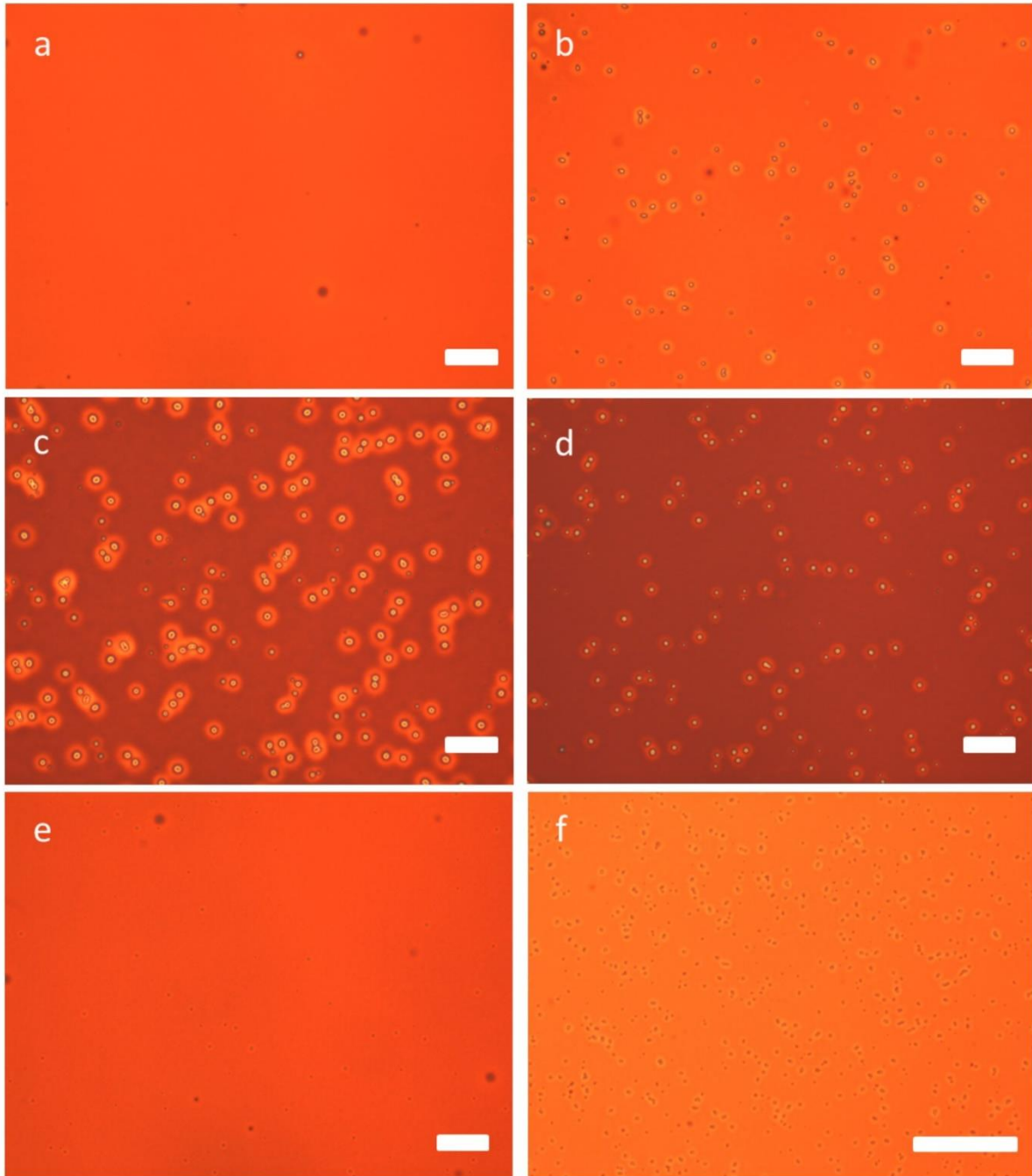
**Fig S14; PCBM/5k-PS fit parameters versus time (6 adjustable parameters in all fits);** a) Bottom layer SLD; b) Sample surface roughness. The kinetic fit parameters all correspond to 2 min time slices. These parameters accompany the other four fit parameters that are shown in figs 3g-3i in the main paper.



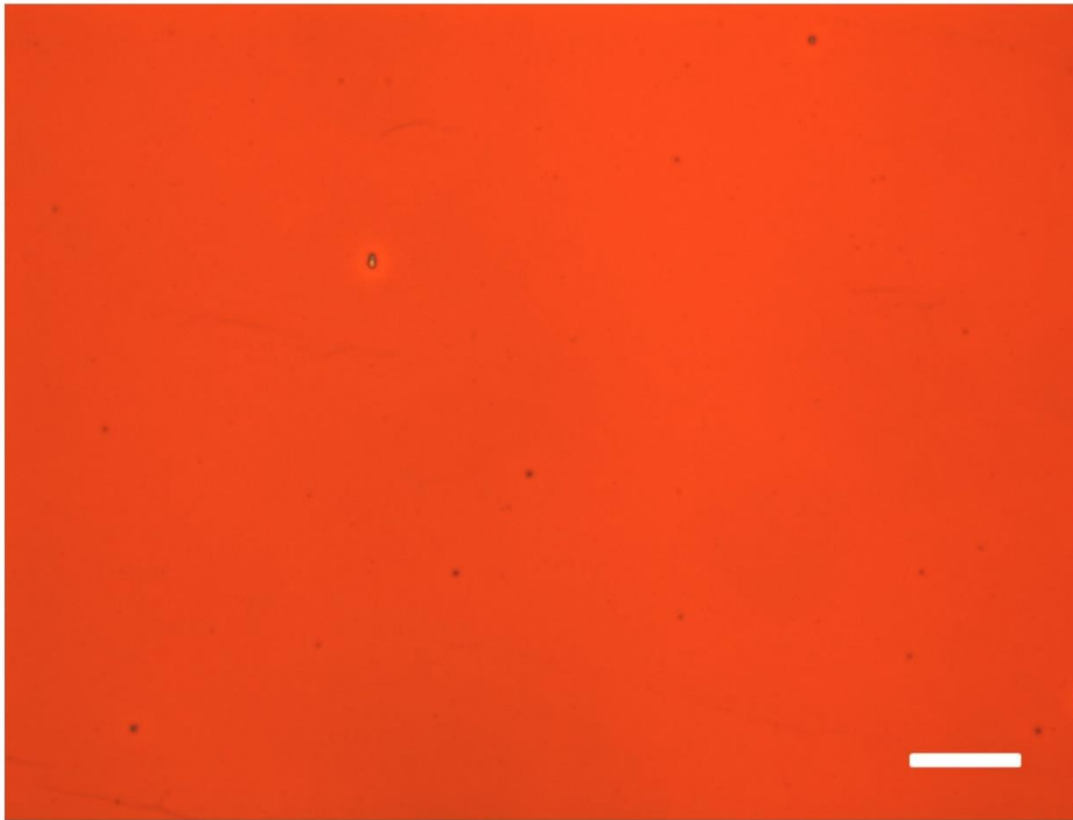
**Fig S15; PCBM/5k-PS kinetic fit parameters versus time for the cases where all 6 parameters are adjustable in comparison to fits in which the sample surface roughness is fixed at 0Å, 10Å and 20Å; a) Top and bottom layer thickness; b) Top layer SLD; c) Interfacial roughness; d) Bottom layer SLD. All fit parameters correspond to 2 min time slices.**

Figure S16 shows optical microscopy images from the *in-situ* annealed PCBM/PS samples in comparison to those from two samples that were *ex-situ* annealed. The images in figs S16a and b show the range of lateral inhomogeneities (fullerene aggregates or small crystallites) that were found on the *ex-situ* annealed samples. As discussed in Hynes et al (supplementary information section S2.3.3)<sup>3</sup>, this level of inhomogeneity does not affect the NR measurements, with the samples shown in S16a and b having very similar reflectivity curves and composition profiles. The inhomogeneities in fig. S16c (*in-situ* annealed 2k-PS/PCBM) cover a larger lateral area than for the *ex-situ* samples and the inhomogeneities also have a larger height (atomic force microscopy shows that the inhomogeneities in fig S16c are around 300-500nm high, in comparison to heights of order 100nm or lower for typical inhomogeneities found in the *ex-situ* annealed samples<sup>3</sup>). As discussed in the main paper, these inhomogeneities appear to be the cause of the failure to fully reproduce the NR measurements using a bilayer model (fig. 1b) and return a reliable interfacial roughness parameter. The inhomogeneities are noticeably smaller in the higher Mw samples shown in figs S16 e and f and also in fig S17 (the bis-PCBM/100-k PS bilayer). The inhomogeneities on the 3k-PS/PCBM bilayer in fig. S16d are intermediate in size between that of the 2k-PS/PCBM and the 5k-PS/PCBM bilayer (fig. S16e). The inhomogeneities on the 20k-PS/PCBM bilayer (fig. S16f), while individually being of small size in comparison to the 2k or 3k bilayers, do have a relatively high density (in comparison to the 5k-PS bilayer). This is potentially because this sample was heated to a higher temperature (and therefore has been annealed for 15-20 min longer at elevated temperature than the lower Mw samples). The relatively high density of the inhomogeneities on the 20k-PS sample may explain why bilayer fits to the kinetic measurements on this sample suffer from

non-uniqueness during fitting with six adjustable parameters (shown in figs S9a and f). It is instructive to note, however, that even this relatively high density of lateral inhomogeneities does not perturb the extracted SLD profile very much in comparison to measurements on *ex-situ* annealed samples, which contain very few lateral inhomogeneities (see Hynes *et al*<sup>3</sup>). This is likely due to the reflectivity from the sample shown in fig. S16f being dominated by the high reflectance from bilayer-like regions between the lateral inhomogeneities.



**Fig S16; Optical micrographs showing typical levels of lateral inhomogeneities on *ex-situ* and *in-situ* annealed PCBM/PS bilayers;** a) A PCBM/5k-PS sample annealed *ex-situ* for 1 minute at 145 °C; b) A PCBM/5k-PS sample annealed *ex-situ* for 5 minutes at 145 °C. Samples c)-f) show samples after *in-situ* annealing; c) PCBM/2k-PS; d) PCBM/3k-PS; e) PCBM/5k-PS; f) PCBM/20k-PS. All scale bars are 30  $\mu\text{m}$ . The two *ex-situ* annealed samples shown in a) and b) have very similar reflectivity curves and fitted SLD profiles (see Hynes *et al*<sup>3</sup> fig. 3 and supplementary figures 5 and 6).



**Fig S17; An optical micrograph showing the typical level of lateral inhomogeneities on the *in-situ* annealed bis-PCBM/100k-PS bilayer. The scale bar is 30 $\mu$ m.**

### **References for supplementary information;**

1. Keddie, J.L., Jones, R.A.L. & Cory, R.A. Size-Dependent Depression of the Glass-Transition Temperature in Polymer-Films. *Europhysics Letters* **27**, 59-64 (1994).
2. Hynes, E.L. Mixing and interfacial composition in polymer/fullerene thin films. PhD thesis, Swansea University (2018).
3. Hynes, E.L. *et al.* Interfacial width and phase equilibrium in polymer-fullerene thin-films. *Communications Physics* **2**, 112 (2019).